# NASA TECHNICAL MEMORANDUM

N 65 - 35 316

(ACCESSION NUMBER)

(PAGES)

(NASA CR OR TMX OR AD NUMBER)

(THRU)

(CODE)

(CATEGORY)

FACILITY FORM 602

# EXPERIMENTAL INVESTIGATION OF MERCURY CONDENSING PRESSURE DROPS

by

M. Gutstein
Lewis Research Center

R. T. Wainwright
Lewis Research Center

A. Koestel
Thompson Ramo Wooldridge, Inc.

GPO PRICE        $ _____

CSFTI PRICE(S) $ _____

Hard copy (HC) _____

Microfiche (MF) _____

ff 653 July 65

NATIONAL AERONAUTICS AND SPACE ADMINISTRATION · WASHINGTON, D.C. · 1964

TECHNICAL MEMORANDUM

EXPERIMENTAL INVESTIGATION OF MERCURY

CONDENSING PRESSURE DROPS

by

M. Gutstein
Lewis Research Center

R. T. Wainwright
Lewis Research Center

and

A. Koestel
Thompson Ramo Wooldridge, Inc.

NATIONAL AERONAUTICS AND SPACE ADMINISTRATION

# EXPERIMENTAL INVESTIGATION OF MERCURY CONDENSING PRESSURE DROPS

by

M. Gutstein
Lewis Research Center

R. T. Wainwright
Lewis Research Center

and

A. Koestel
Thompson Ramo Wooldridge, Inc.
Cleveland, Ohio

## ABSTRACT

Experiments are described wherein the local static pressures were measured along tubes in which mercury vapor was flowing and condensing. Data were obtained at flow rates of 1.05 to 3 lb/min, at inlet pressures of 8 to 30 psia, and at condensing lengths of 4 to 8 ft. Both constant diameter and tapered tubes were employed in the study.

A comparison of the two-phase frictional pressure drop with the Lockhart-Martinelli correlation showed significant deviations, particularly at low qualities. A relation between the frictional pressure drop and the Weber number, derived from fog-flow considerations, correlated the trend of the data over the full quality range. Experimental data obtained from the literature were utilized to further support this fog-flow correlation.

## INTRODUCTION

Rankine cycle powerplants utilizing mercury as a working fluid are being considered for space applications. Inherent in the performance of such plants is the need to condense the effluent of the turbine, that is, the mercury vapor. In a powerplant for space, this process might occur

X-52034

inside tubes, and the heat of condensation would be dissipated by radiation. To specify the dimensions of the tubes, their diameter, length, taper, etc., requires accurate prediction of the pressure drops associated with mercury condensing at low heat fluxes. In recognition that such predictions are not available, experiments were performed to measure the local static pressures along tubes of constant and varying diameter in both the wetting and nonwetting regimes. Moreover, an analysis of the fluid mechanics of condensing mercury was undertaken to develop a means to predict these pressure drops. A preliminary review of these efforts was previously given in Ref. 1 and is discussed in detail in the present paper.

A veritable literature exists today that describes, predicts, and correlates two-phase frictional pressure gradients. For condensation, however, and for mercury condensation in particular, the correlation of Lockhart-Martinelli (2) and its refinement, the correlation of Baroczy and Sanders (3) are of most significance. The Lockhart-Martinelli approach consists of equating the pressure gradients obtained from adiabatic, two-component flows to the case of condensation at the equivalent liquid to vapor superficial pressure gradient ratios. The total frictional pressure difference across a condenser tube may then be obtained by integration of the local gradients. The work of Baroczy and Sanders constituted an improvement to this correlation by accounting for a vapor Reynolds number effect that they observed in experiments with the adiabatic flow of mercury and nitrogen.

Hays (4) applied these correlations to mercury condensation data and found general agreement to within about ±25 percent. However, at low heat

rejection rates or at low qualities (low vapor Reynolds numbers), Hays con-
concluded that agreement of the test results with these correlations was
not apparent. The author attributed this finding to fog flow and believed
the Lockhart-Martinelli correlation to be inapplicable to this flow regime.

Kiraly (5) presents a comparison of two-phase mercury-nitrogen pres-
sure differences with the Martinelli curve. He likewise compares overall
pressure differences of mercury condensation in horizontal tubes with the
same correlation. In both cases agreement is good. However, condensation
inside horizontal tapered tubes and inclined tubes of constant diameter
showed considerable deviation. Thus it appears that the Lockhart-Martinelli
correlation does not satisfactorily predict the pressure gradients of mer-
cury condensation at low vapor velocities and low heat fluxes or those for
unusual geometries and orientations. This conclusion implies that the pres-
sure drops for mercury condensation should be distinguished from those ob-
tained from adiabatic experiments.

The authors also compared their experimental data with Lockhart-
Martinelli and likewise found significant deviations, particularly at low
qualities. The trends of the data, however, were predicted by an analysis
of pressure differences based on the flow of a mixture of entrained drops
and vapor through a passage formed by stationary wall-adhering drops. This
particular fog-flow pattern may be for nonwetting fluids analogous to the
spray-annular regime of wetting fluids to which the Lockhart-Martinelli
correlation is known to be inapplicable (6,7). The pressure drop data,
which were obtained when the mercury seemingly wetted the tube wall, were
also correlated by the fog-flow theory; the true flow regime for this mode

of mercury condensation therefore remains uncertain. A discussion of these matters is presented herein.

## DESCRIPTION OF EQUIPMENT AND PROCEDURE

Equipment. The mercury condensing experiments were conducted in a closed, natural circulation test loop shown schematically in Fig. 1. Fabricated entirely of stainless steel except for some of the condenser test sections, the rig consisted of a mercury pot boiler, a superheater section, and a flow metering unit. Each condenser test-section tube was welded into the rig between the superheater and the flow meter. Brief descriptions of these components are now presented.

The pot boiler consisted of an 8-in.-diameter by 9.75-in.-tall cylinder partially immersed in an electrically heated salt bath. A baffle-cup arrangement was provided at the top of the boiler (at the entrance to the superheater) to separate and recirculate any liquid mercury entrained in the vapor. The salt bath heaters were capable of generating a maximum of 9 kw of heat at bath temperatures up to about 1000 F.

The superheater was an electrically heated L-shaped tube that extended from the top of the boiler to the inlet of the test section. The vertical portion was 4 ft long and 1 in. in diameter. The horizontal portion was 1 ft long. Its inner diameter was machined to match the inlet internal diameter of each test section, thereby minimizing flow disturbances. The electric heater that was wrapped entirely about this component of the rig was capable of generating 4.5 kw and was employed to slightly superheat the vapor. Thus, any entrained liquid that managed to enter the superheater was probably vaporized.

Four condenser test sections, including both constant diameter and tapered tubes, were employed in this investigation. Their geometry and materials of construction are described in Table I. The range of such experimental variables as the flow rate, the inlet pressure, the inlet vapor velocity, etc. are likewise listed in this table. Static-pressure taps at intervals of every 14 to 18 in. along the tube length were provided each test section. These taps consisted of lengths of stainless-steel tubing, 0.085-in. inner diameter, connected directly to stainless-steel mercury manometers. The low-pressure sides of the manometers were made of transparent plastic tubing. One of these manometers measured the static pressure at the test-section inlet relative to atmospheric pressure. The remaining manometers were connected to a common manifold and were used to measure relative static pressures.

Each test section was cooled by a crossflow of air from two diametrically opposed plenums. Because the air heat-transfer coefficient was controlling, the heat flux was essentially constant over the full length of the tube. A maximum heat flux of about 40,000 Btu/(hr)(sq ft) was attainable.

The major features of the condensing process that occurred inside the test sections were observed with an X-ray unit and fluorescope screen. This combination was mounted on a track and could traverse the entire test-section length. It was also employed to check the mercury level in the manometer taps at the junction to the test section and to detect the presence of large quantities of noncondensible gases downstream of the interface.

The mercury flow rate was measured by timing the collection of a known

volume of condensate in a glass vessel located between the test section and the boiler. Care was taken to preserve the steady-state condition of the rig during a flow measurement.

Operation. Prior to start-up, the levels of mercury and molten salt were carefully adjusted to insure a steady boiling process. Previous experience with the rig had shown that too low a salt level prevented the attainment of the higher vapor flow rates because of insufficient boiler heat-transfer area. Too high a mercury level often caused severe pressure oscillations.

At start-up the manometer lines were closed and the rig was evacuated. The salt bath heaters were then energized and the flow of cooling air was initiated. Once a steady flow of mercury vapor was obtained, the manometers were opened. Noncondensible gases were continuously removed by a vacuum pump until X-ray examination of the interface no longer indicated their presence. Thereafter the tube wall temperature immediately upstream of the interface was used to monitor the presence of noncondensibles. Whenever this temperature was well below the average condenser wall temperature, it indicated the collection of these gases at this location.

Data were recorded after attaining a steady-state condition that was defined by the constancy, for a period of at least 15 min, of the manometer levels, the boiler, the salt bath and wall temperatures, and the vapor-liquid interface position.

ANALYSIS OF EXPERIMENTAL DATA

The pressure, flow rate, and condensing length data obtained in this investigation are presented in Ref. 8.

Figure 2 illustrates a typical static pressure profile along the test section. The rise or recovery of the static pressure toward the outlet of the test section, as shown in this figure, is characteristic of condensing and is attributable to the effect of net momentum changes. These momentum changes have to be estimated in order to obtain the two-phase frictional pressure drops. A description of the method used to calculate the momentum changes is now presented.

The static pressure difference measured between two taps of a horizontal, constant diameter tube in which condensing occurs is given by the expression

$$dP_s = dP_{TPF} + dP_{mo} \tag{1}$$

It can be shown that the $dP_{mo}$ term can be expanded to give

$$dP_s = dP_{TPF} + \frac{G_T^2}{g} \left\{ d\left[ \frac{(1 - x)^2}{\rho_f R_f} \right] + d\left( \frac{x^2}{\rho_v R_v} \right) \right\} \tag{2}$$

Equation (2) indicates that the friction component of the static pressure difference can be obtained only when the volume fractions (or local slip ratios, $U_f/U_v$ [*]) are known. Presently the only correlation of mercury

---

[*]The slip ratio is related to the volume fraction by

$$R_v = 1 \left/ \left( \frac{1 - x}{x} \frac{\rho_v}{\rho_f} \frac{U_v}{U_f} + 1 \right) \right.$$

It should be noted that $R_f$ does not include the stationary liquid drops at the wall. Experimental measurements of $R_f$ must therefore distinguish between the moving and the stationary liquid.

volume fractions available is that derived from adiabatic nitrogen-mercury measurements as reported by Baroczy (9). This correlation is believed inapplicable to the case of mercury condensing for reasons which are discussed in Ref. 1. Hays (4) reported frictional pressure gradients of condensing mercury for two limiting cases, those of a slip ratio of zero and one. Hays further recommended a slip of zero based on photographic evidence and the agreement of his data with the Lockhart-Martinelli correlation. However, as mentioned previously, deviations from this correlation were noted, particularly at low heat fluxes. These deviations were attributed to the presence of fog-flow (i.e., slip ratios of approximately one).

Figure 3 presents the frictional pressure gradients obtained from the data of Fig. 2, calculated on the basis of slip ratios of both zero and one. Significantly different gradients can clearly be obtained depending on the value of the slip chosen.

The authors assumed a value of the slip ratio of one to obtain the frictional pressure gradients from their experimental data. This assumption was supported by the following evidence: Observations of the condensing process by means of the X-ray indicated that the predominant flow regime for low-heat-flux mercury condensation appeared to be that of a dispersion of fine drops flowing with the vapor, the regime frequently called "fog-flow." The assumption of a slip of one for this regime is considered reasonable. Furthermore, an analysis was performed to predict the velocity and position of mercury drops entrained and flowing in a vapor stream. Figure 4 shows a typical result of this analysis. The velocity of

drops entrained at positions corresponding to the inlet and 0.2, 0.4, 0.6, and 0.8 of the condensing length are plotted along with the vapor velocity distribution. This graph indicates that most drops are rapidly accelerated to very nearly the local gas velocity, and that the drops then follow this velocity even though it diminishes because of condensation. Only drops entrained near the interface, such as at the position corresponding to 0.8 of the condensing length, do not possess a slip ratio approximating one. Even so, the drops that were entrained upstream of this position and that constitute the bulk of the liquid phase in the vapor at this position all possess slip ratios very nearly equal to one. Further details of this analysis are given in Ref. 8. Finally, the assumption of a slip of one was borne out by the general correlation of the frictional-pressure-drop data with the fog-flow analysis presented in Appendix B. A discussion of this correlation is presented in the section FOG-FLOW CORRELATION OF NON-WETTING DATA of this report.

## DISCUSSION OF RESULTS

Empirical Correlation of Nonwetting Data. A correlation of adiabatic, two-component, two-phase frictional pressure drops was proposed by Lockhart and Martinelli (2). This frequently cited correlation presented a relation between the parameters $\Phi_v^2$ and $X$ defined as follows:

$$\Phi_v^2 = \left(\frac{\Delta P}{\Delta L}\right)_{TPF} \bigg/ \left(\frac{\Delta P}{\Delta L}\right)_v$$

$$X = \sqrt{\left(\frac{\Delta P}{\Delta L}\right)_f \bigg/ \left(\frac{\Delta P}{\Delta L}\right)_v}$$

Four flow regimes were also distinguished in accordance with the values

of the superficial Reynolds numbers of the phases. Of these, only the

viscous liquid - viscous vapor regime was not encountered in the mercury

condensing experiments.

Figure 5 presents the Lockhart-Martinelli curves and the data of

Series F, typical of the nonwetting condensing experiments. Examination

of this graph shows that the Lockhart-Martinelli correlation appears to

predict the data only at the high-quality region (i.e., low values of X).

At low qualities the data deviate considerably from the correlation;

furthermore, the data do not seem to segregate by flow regime in the man-

ner suggested by Lockhart-Martinelli.

The modified version of the Lockhart-Martinelli correlation by Baroczy

and Sanders (3) was found likewise not to correlate the mercury condensing

data. In general, the experimentally determined pressure drops were larger

than the predicted ones, and a clear vapor Reynolds number effect could

not be established. A similar conclusion was drawn by Hays (4).

Fog-Flow Correlation of Nonwetting Data. Appendix A presents in de-

tail a description of the fog-flow regime believed to be predominant in

nonwetting mercury condensation. This description forms the basis of the

theory that is derived in Appendix B. A brief summary of both the flow

model and the analysis is presented below as well as a comparison of pre-

dicted and experimentally determined pressure drops.

X-ray examination of the condenser test sections indicated that for

nonwetting condensing, drops are formed at the heat-transfer surface and

grow until they are displaced and entrained into the vapor stream. The

mixture of entrained drops and vapor therefore flows through a passage

formed by the stationary, wall-adhering drops. The diameter of this pas-

sage $D_m$ is less than the tube diameter $D_T$ by twice the thickness of

the drop layer. Application of the Fanning equation for frictional pres-

sure drop due to a homogeneous or fog-flow dispersion gave the following

result in terms of the Lockhart-Martinelli parameter $\Phi_v^2$, the quality,

and the ratio of the diameters:

$$\Phi_v^2 x^{3/4} = \left(\frac{D_T}{D_m}\right)^{4.75} \tag{B11}$$

Likewise, by assuming the drop layer thickness to be equal to the diameter

of drops at incipient entrainment, a relation was derived between the

Weber number (based on the superficial vapor velocity) and the ratio of

the diameters as shown below.

$$\frac{D_T \rho_v U_v^2}{2 g_c \sigma} = \frac{0.371^\dagger}{\left(\frac{D_T}{D_m}\right)^4 - \left(\frac{D_T}{D_m}\right)^3} \tag{B19}$$

Thus by selecting values of the ratio $D_T/D_m$, the relation between

$\Phi_v^2 x^{3/4}$ and the local Weber number was obtained. This relation is plotted

as the curves of Figs. 6 through 9. The experimental values of these pa-

rameters are also plotted on these graphs for confirmation of the fog-flow

theory. A typical calculation of the parameters $\Phi_v^2 x^{3/4}$ and the Weber

number is illustrated in Ref. 8 for the tapered test section.

Figures 6 through 9 compare the pressure drop data of Series A, D, E,

and F, respectively, with the fog-flow theory (see Table I). These graphs

---

$\dagger$The constant 0.371 was determined by experiments with single mercury

drops on a flat inclined plate (see Appendix B).

show that at Weber numbers greater than about 10, the experimental values

of $\Phi_v^2 x^{3/4}$ seem to equal one and are independent of the Weber number (i.e.,

the thickness of the drop layer is very nearly negligible). At lower values

of the Weber number, $\Phi_v^2 x^{3/4}$ becomes significantly greater than one and de-

pendent on the Weber number. Although considerable scatter is present, the

fog-flow theory predicted this trend of the data. The greater scatter of

the data for the Series E tests was attributed to the larger tube diameter

and the consequent difficulty in measuring the smaller frictional pressure

drops or to a deviation from fog-flow due to the lower vapor velocities.

COMPARISON OF THEORY WITH NONWETTING DATA OF OTHER EXPERIMENTERS

Data of Hays. The partial and total condensation of mercury vapor in

glass and metal tubes of relatively small diameter and short length was

studied by Hays (4). The range of variables of these experiments is listed

in Table II. Figure 10 presents the data and the theoretical fog-flow

prediction. The authors believe that further corroboration of the fog-

flow model is afforded by these data.

Data of Albers, et al. Local mercury condensing pressure drops were

measured in a constant diameter and a tapered tube by Albers, et al. (10,

11). The data were obtained in normal-gravity and zero-gravity environ-

ments, the latter by flying zero-gravity trajectories in an airplane. The

geometries and approximate range of variables are given in Table III. Fig-

ures 11 and 12 present the data of these experiments as well as the pres-

sure drops predicted by the fog-flow theory. Although the constant diameter

tube data of Fig. 11 seem to be satisfactorily correlated by the theory,

the tapered tube data are scattered. An explanation for this scatter has

not been determined.

## CORRELATION OF WETTING DATA

Prolonged testing with the constant diameter tube of Series A caused the mercury to wet the condensing surface. The data that were recorded during this condition were reported as the Series W experiments. To explore this phenomenon in greater detail, the Series G tests were performed with magnesium and titanium added to the mercury to induce wetting. Both the Series W and G experiments were characterized by elongated interfaces, as shown in Fig. 13, as opposed to the more or less vertical interfaces present in the nonwetting tests.

Figure 14 presents the Series G data plotted in accordance with the Lockhart-Martinelli correlation. Comparison of this graph with that shown in Fig. 5 illustrates an unusual similarity between the wetting and nonwetting two-phase frictional pressure differences. This similarity is further indicated by the graphs of Figs. 15 and 16 in which the Series W and G data are correlated with the fog-flow parameters. That the fog-flow theory predicts the pressure-drop trends for the wetting condensation is probably explained by one of the following two possibilities: The degree of wetting induced by the additivies may have been limited and the condensation may still have been essentially dropwise, or, on the other hand, wetting may actually have been the mode of condensation. If the latter were true, the results of Figs. 15 and 16 would indicate that the fog regime was still present, but a liquid film rather than a drop layer covered the inner surface of the tube (i.e., spray-annular flow regime). Moreover, this film must have behaved very much like the drop layer; that is, the thickness of the layer and its surface roughness had to be comparable and

the drops entrained from the film had to be similar in number and size at incipient entrainment to the nonwetting entrained drops. Koestel and Smith (12) analyzed the spray-annular flow regime and, by application of film stability considerations, likewise achieved correlation of the Series G data. Thus further experimental work and analyses are required to determine which of these flow models, the fog-flow regime with stationary wall drops or the spray-annular film regime, more accurately describes the flow pattern for wetting mercury condensation.

## SUMMARY AND RECOMMENDATIONS

The experimental equipment used to measure local static pressure drops for low-heat-flux mercury condensation was described. The frictional pressure drops that were obtained were shown to be inadequately predicted by the Lockhart-Martinelli correlation, particularly at low qualities. A fog-flow theory was formulated, which was inferred from observations of the flow regime. A relation was obtained between the Weber number (based on the superficial vapor velocity) and the fog-flow parameter $\Phi_v^2 x^{3/4}$. Comparison of condensing mercury data obtained by the authors and other experimenters with this fog-flow relation showed that the theory satisfactorily predicted the trends of these data over a wide range of test conditions.

The authors recommend that future studies of mercury condensation determine the limits of the fog-flow theory since the application of the theory to condensation at higher heat fluxes and to the situation of wetting fluids is as yet uncertain. Finally, future investigations should include a study of the flow regimes encountered and a careful determination of the liquid volume fractions, both of which are essential to a complete understanding of the physics of condensation.

## ACKNOWLEDGMENT

APPENDIX A

DESCRIPTION OF THE FLOW REGIME

Fundamental to the prediction of two-phase pressure drop or heat transfer is a knowledge of the existing flow regime. For the case of condensation occurring inside tubes, wetting fluids generally form a thin annular layer at the heat-transfer surface. In all likelihood drops are sometimes broken from this film and are entrained in the vapor core. For mercury condensation, however, a continuous liquid film is difficult to obtain even when the mercury wets its container. More typically a layer of drops is formed at the tube wall. The greater portion of the condensate is then transported to the tube exit by the entrainment of these drops into the vapor stream. At relatively high vapor velocities this two-phase flow has been observed and described as a "fog-flow" (13). Even at lower vapor flow rates the "fog" regime is probably present although gravity effects, such as large agglomerated drops, do appear. A more detailed picture of the fog-flow regime of mercury condensation is offered below for the purpose of deriving a two-phase frictional-pressure-drop prediction.

The authors postulate that the drops entrained into the vapor stream are extremely small (of the order of 0.001- to 0.010-in. diameter) and are rapidly accelerated to very nearly the local vapor velocity. The drops are further conceived to respond to the turbulent fluctuations of the vapor phase and are dispersed so that the effects of concentration gradients are negligible. In effect, the drops travel with and become a part of the vapor stream; the two-phase mixture is thus assumed to behave as a single-phase fluid.

This liquid-vapor fog flows through the passage formed by the drops that are attached to the tube wall. The passage, however, is essentially hydraulically smooth because of the close packing of the drops on the wall. (Experimental confirmation of the existence of such a characteristic was presented in Ref. 1) It is further assumed that increasing the packing of the drops at the wall by raising the heat flux would have little or no effect on the friction factor. The diameter of the duct through which the fog-like mixture flows is $D_T - 2\delta_D$, where $\delta_D$ is the effective thickness of the drop layer at a particular location.

In a previous study performed by Denington, et al. (14) it was shown that the diameter of mercury drops that were entrained into a flowing nitrogen stream was related to the velocity of the gas. It is suggested that such a relation also exists for mercury condensing: a drop grows to a particular size called the critical drop diameter (defined by the velocity of the vapor) and is then entrained into the vapor core. The effective thickness of the drop layer on the wall at a particular position was therefore taken as equal to the critical drop diameter at that position. Thus, the vapor velocity (here, the velocity of the fog) determines the thickness of the condensate layer at the wall and is, in turn, dependent on this thickness by continuity. The prediction of the frictional pressure gradients for condensing mercury based on the previous considerations is in Appendix B.

## APPENDIX B

## DERIVATION OF THE FOG-FLOW THEORY

<u>Critical Drop Size</u>. Reference 14 presents a detailed experimental
and theoretical analysis of the entrainment of mercury drops. A brief
review of this work as it applies to mercury condensation is presented
below, since the mechanics of this process forms an important part of
the fog-flow model.

As a drop forms and grows on a tube surface, forces are produced
that tend either to make the drop move or to oppose its movement. These
forces consist of the drag caused by the flowing vapor, the gravity force,
and the interfacial force between the drop and the wall arising from the
deformation of the drop by either of the two previous forces. At a partic-
ular drop size, the critical drop diameter $\delta_{cr}$, these forces are no longer
balanced and the drop is displaced. Thus, at incipient movement, the fol-
lowing force balance must be applicable:

<p align="center">Drag Force ± Gravity Force - Interfacial Force = 0</p>

or

$$\frac{\pi\delta_{cr}^2}{4} \frac{C_{d,\delta} \rho_v U_v^2}{2g_c} \pm n(\sin \theta)\rho_f \frac{\pi\delta_{cr}^3}{6} - \pi\delta_{cr}\sigma E_\sigma = 0 \qquad (B1)$$

where

$C_{d,\delta}$    drag coefficient for drop

$n$    ratio, $g/g_c$

$\sigma$    surface tension

$E_\sigma$    constant, accounts for effects of drop deformation, contact angle,
      and surface condition, $<1$

The coefficient of drag for drops $C_{d,\delta}$ is also dependent on the deformation. In general, the coefficients for deformable bodies (bubbles, drops, etc.) are greater than for solid spheres and have values very nearly equal to one (15). For simplicity, the coefficients may be assumed equal to one and the value of $E_\sigma$ can be made to accommodate the deformation effect. Thus, in horizontal tubes or in the absence of a gravitational field, the critical drop size is related to the vapor velocity as follows:

$$\frac{\delta_{cr}\rho_v U_v^2}{2g_c\sigma} = 4E_\sigma \qquad (B2)$$

The term on the left side of Eq. (B2) is the Weber number for the drop. Through experiments conducted both in tubes and with inclined flat plates, $E_\sigma$ was found to have the value of 0.0464. For a more detailed discussion of these experiments and their analysis, Ref. 14 should be consulted.

Derivation of the Fog-Flow Model. If the discussion of the previous sections truly describes the flow regime for mercury condensing inside tubes, then the frictional component of the static pressure drop may be written as a single equation for both phases as follows:

$$\left(\frac{dP}{dL}\right)_{TPF} = \frac{f_m W_m^2}{2g_c D_m \rho_m \left(\frac{\pi}{4} D_m^2\right)^2} \qquad (B3)^\ddagger$$

---

[‡] Equation (B3) of the derivation assumes a homogeneous flow or a fog-flow. An entirely similar expression was used by Owens (16) in calculating the pressure drops for air-water and steam-water mixtures. Comparison of his predictions with the Martinelli-Nelson correlation (17) gave reasonable agreement. Inasmuch as the Martinelli-Nelson correlation was based on Lockhart-Martinelli, it is therefore likely that the latter will correlate

where

$f_m$    friction factor for fog mixture

$D_m$    diameter of flow passage formed by drops on wall through which fog

      flows

The frictional pressure drop that would result if the vapor portion of the

fog were to flow through the bare pipe is

$$\left(\frac{dP}{dL}\right)_v = \frac{f_v(xW_m)^2}{2g_c D_T \rho_v \left(\frac{\pi}{4} D_T^2\right)^2}$$ (B4)

The Lockhart-Martinelli modulus $\Phi_v^2$, defined as the ratio of the two

gradients, is therefore

$$\Phi_v^2 = \frac{f_m}{f_v} \frac{1}{x^2} \frac{\rho_v}{\rho_m} \left(\frac{D_T}{D_m}\right)^5$$ (B5)

The friction factor for turbulent flow in smooth passages is given by

$$f_m = \frac{0.316}{(N_{Re,m})^{0.25}} = \frac{0.316}{\left(\frac{4W_m}{\pi D_m \mu_m}\right)^{0.25}}$$ (B6)[§]

___

the pressure drops of a fog-flow that completely fills its passage, that

is, in which there is no annular liquid layer. Such a condition is appar-

ently approached in mercury condensation at Weber numbers greater than

about 10, corresponding to values of X of less than about 0.04. Fig-

ure 5 shows that the Lockhart-Martinelli correlation does indeed seem to

predict the pressure drops of this flow regime for the Series F data.

[§]These expressions assume turbulent flow. Reference 1 presents over-

all mercury condensing pressure drops for laminar flow conditions correlated

by the fog-flow theory assuming $f = 64/N_{Re}$.

and

$$f_v = \frac{0.316}{(N_{Re,v})^{0.25}} = \frac{0.316}{\left(\dfrac{4xW_m}{\pi D_T \mu_v}\right)^{0.25}} \qquad (B7)^{\S}$$

The viscosities $\mu_m$ and $\mu_v$ are transport properties and are more dependent on the volume fraction of the two phases than on the weight fraction. Since the volume fraction of the flowing liquid is much less than one, it can be assumed that

$$\mu_m = \mu_v \qquad (B8)$$

(A similar assumption concerning the viscosities was made by Bankoff (18).) Therefore,

$$\frac{f_m}{f_v} = \left(\frac{D_m x}{D_T}\right)^{0.25} \qquad (B9)$$

The density ratio may be considered to be weight fraction dependent. Thus,

$$\frac{\rho_v}{\rho_m} = x \qquad (B10)$$

Combining Eqs. (B5), (B9), and (B10) gives

$$\Phi_v^2 = \frac{1}{x^{3/4}}\left(\frac{D_T}{D_m}\right)^{4.75} \qquad (B11)$$

A relation between $D_T/D_m$ and the Weber number may be derived for horizontal flow or zero gravity as follows: From Eq. (B2) the Weber number based on the tube diameter may be obtained:

---

§ These expressions assume turbulent flow. Reference 1 presents overall mercury condensing pressure drops for laminar flow conditions correlated by the fog-flow theory assuming $f = 64/N_{Re}$.

$$\frac{D_T \rho_v U_m^2}{2g_c \sigma} = \frac{4E_\sigma D_T}{\delta_{cr}} \qquad (B12)^{\|}$$

Note that the vapor density is employed rather than the mixture density since only the vapor conditions influence the entrainment.

From continuity,

$$\frac{\pi D_T^2}{4} \rho_v U_v = \frac{\pi D_m^2}{4} \rho_v U_m \qquad (B13)$$

where $U_v$ represents the velocity of the vapor in a bare tube with all the liquid removed. Therefore,

$$\left(\frac{D_T}{D_m}\right)^2 U_v = U_m \qquad (B14)$$

Substituting Eq. (B14) into Eq. (B12) yields

$$\frac{D_T \rho_v \left(\frac{D_T}{D_m}\right)^4 U_v^2}{2g_c \sigma} = \frac{4E_\sigma D_T}{\delta_{cr}} \qquad (B15)$$

When the assumption that, at a particular point in the tube, the critical drop diameter corresponds to the effective thickness of the drop layer is utilized,

$$D_T - 2\delta_{cr} = D_m \qquad (B16)$$

or

$$\frac{D_T}{\delta_{cr}} = \frac{2}{1 - \dfrac{D_m}{D_T}} \qquad (B17)$$

Substituting Eq. (B17) into Eq. (B15) yields

---

$^{\|}$Note that for condensing inside inclined tubes in a gravity field, the analysis would proceed from Eq. (B1) rather than from Eq. (B2).

$$\frac{D_T \rho_v U_v^2}{2g_c \sigma} = \frac{4E_\sigma}{\left(\dfrac{D_T}{D_m}\right)^4} \frac{2}{1 - \dfrac{D_m}{D_T}} \tag{B18}$$

or

$$\frac{D_T \rho_v U_v^2}{2g_c \sigma} = \frac{8E_\sigma}{\left(\dfrac{D_T}{D_m}\right)^4 - \left(\dfrac{D_T}{D_m}\right)^3} \tag{B19}$$

Thus from Eqs. (B11) and (B19), a relation has been shown to exist between the Lockhart-Martinelli modulus $\Phi_v^2$ and the Weber number such that

$$\Phi_v^2 x^{3/4} = f\left(\frac{D_T \rho_v U_v^2}{2g_c \sigma}\right) \tag{B20}$$

By assuming values of the ratio $D_T/D_m$, the relation between the Weber number and $\Phi_v^2 x^{3/4}$ may be obtained.

NOMENCLATURE

| | |
|---|---|
| $C_{d,\delta}$ | drag coefficient for mercury drops, dimensionless |
| D | diameter, ft |
| $E_\sigma$ | constant of Eq. (B1), dimensionless |
| G | mass velocity, lb/(hr)(sq ft) |
| L | length, ft |
| $N_{Re}$ | Reynolds number, dimensionless |
| R | volume fraction, dimensionless |
| U | average velocity, ft/sec |
| W | mass flow rate, lb mass/sec |
| dP | increment of pressure |
| f | friction factor, dimensionless |
| g | local gravitational acceleration, ft/sec$^2$ |
| $g_c$ | conversion factor, 32.174 (lb mass)(ft)/(lb force)(sec$^2$) |
| n | ratio, $g/g_c$, lb force/lb mass |
| x | quality, dimensionless |
| $f$ | function of |
| t - t | Lockhart-Martinelli turbulent-liquid - turbulent-gas flow regime |
| t - v | Lockhart-Martinelli turbulent-liquid - viscous-gas flow regime |
| v - t | Lockhart-Martinelli viscous-liquid - turbulent-gas flow regime |
| $\Phi$ | Lockhart-Martinelli parameter |
| X | Lockhart-Martinelli parameter |
| $\delta$ | drop diameter, ft |
| $\theta$ | angle of inclination |
| $\mu$ | viscosity, lb mass/(ft)(sec) |

ρ        density, lb mass/cu ft

σ        surface tension, lb force/ft

Subscripts:

cr      critical

D       effective

f        liquid

m       fog mixture

mo      momentum

s        static

T       total

TPF     two-phase frictional

v       vapor

## REFERENCES

1. A. Koestel, M. Gutstein, and R. T. Wainwright, Fog-Flow Mercury Condensing Pressure Drop Correlation, Presented at Third High-Temperature Liquid Metal Heat Transfer Technology Conference, Oak Ridge National Laboratories, Sept. 4, 1963. (To be pub.)

2. R. W. Lockhart and R. C. Martinelli, Proposed Correlation of Data for Isothermal Two-Phase, Two-Component Flow in Pipes, Chemical Engineering Progress, Vol. 45, No. 1, pages 39-48, 1949.

3. C. J. Baroczy and V. D. Sanders, Pressure Drop for Flowing Vapors Condensing in a Straight Horizontal Tube, Atomics International Special Report NAA-SR-6333, June 1, 1961.

4. L. Hays, Investigation of Condensers Applicable to Space Power Systems. Part I. Direct Condensers, Electro Optical Systems, Inc. Report 1588, September 10, 1962.

5. R. Kiraly and A. Koestel, The SNAP-2 Power Conversion System Topical Report No. 8, Condenser Development and Design Study, Thompson Ramo Wooldridge, Inc. Report No. ER-4104, June 30, 1960.

6. C. J. Hoogendoorn, Gas-Liquid Flow in Horizontal Pipes, Chemical Engineering Science, vol. 9, no. 4, Feb. 1959, pages 205-217.

7. S. Chien, An Experimental Investigation of the Liquid Film Structure and Pressure Drop of Vertical, Downward, Annular, Two-Phase Flow, Ph.D. Dissertation, University of Minnesota, April 1961.

8. A. Koestel, et al., Mercury Wetting and Non-Wetting Condensing Research, Thompson Ramo Wooldridge, Inc. Final Report on Contract NAS3-2159. (To be pub.)

9. C. J. Baroczy, Correlation of Liquid Fraction in Two-Phase Flow with Application to Liquid Metals, Atomics International Special Report NAA-SR-8171, April 15, 1963.

10. J. Albers, R. Macosko, and C. Crabs, An Experimental Pressure Drop Investigation of Mercury Condensing in a Constant Diameter Tube in One-G and Zero-G Environments, Proposed NASA Technical Note.

11. J. Albers and R. Macosko, An Experimental Pressure Drop Investigation of Mercury Condensing in a Tapered Tube in a One-G and Zero-G Environment, Proposed NASA Technical Note.

12. A. Koestel and C. Smith, Radiator Design Limitations for Dynamic Converters, Paper Presented at Sixth AGARD Combustion and Prop. Colloquium, Cannes (France), Mar. 16-20, 1964.

13. R. Gido and A. Koestel, Mercury Wetting and Non-wetting Condensing Research, Thompson Ramo Wooldridge, Inc. Progress Report No. ER-5214, January 1963.

14. R. J. Denington, et al., Space Radiator Study, Thompson Ramo Wooldridge, Inc. Report ER-4544, April 30, 1962.

15. R. R. Hughes and E. R. Gilliland, The Mechanics of Drops, Chemical Engineering Progress, vol. 48, no. 10, page 497-505, October 1952.

16. W. L. Owens, Jr., Two-Phase Pressure Gradient, International Developments in Heat Transfer. Proc. 1961-1962 Heat Transfer Conference, ASME, 1963, pp. 382-390.

17. R. C. Martinelli and D. B. Nelson, Prediction of Pressure Drop During Forced-Circulation Boiling of Water, ASME, Trans., vol. 70, no. 6, page 695-702, August 1948.

18. S. G. Bankoff, A Variable Density Single-Fluid Model for Two-Phase
Flow with Particular Reference to Steam-Water Flow, Journal of Heat
Transfer, Transactions of ASME, Series C, Vol. 82, pages 265-272,
1960.

TABLE I. - RANGE OF VARIABLES FOR MERCURY CONDENSING EXPERIMENTS

| Variable | Series A | Series F | Series E | Series W | Series G | Series D |
|---|---|---|---|---|---|---|
| Condensing length, in. | 94 | 53 - 94 | 48 - 95 | 94 | 53 - 94 | 48 - 82 |
| Tube diameter, in. | 0.319 | 0.319 | 0.397 | 0.319 | 0.319 | 0.4 × 0.2 |
| Tube material | 316 SS | Haynes 25 | Haynes 25 | 316 SS | Haynes 25 | Haynes 25 |
| Vapor inlet pressure, psia | 8.0 - 30.2 | 12.1 - 30.4 | 11.4 - 30.4 | 19.6 - 20.2 | 10.6 - 30.5 | 14.9 - 30.1 |
| Vapor inlet quality | 1.0 | 1.0 | 1.0 | 1.0 | 1.0 | 1.0 |
| Vapor inlet velocity, ft/sec | 114 - 278 | 82 - 302 | 50.238 | 152 - 200 | 74 - 291 | 86 - 195 |
| Vapor inlet Reynolds number | 477 - 50,000 | 833 - 43,159 | 706 - 36,096 | 700 - 36,000 | 808 - 40,000 | 1670 - 39,200 |
| Mass flow rate, lb/min | 1.09 - 3.12 | 1.18 - 2.36 | 1.12 - 2.40 | 1.64 - 2.14 | 1.05 - 2.36 | 1.41 - 2.91 |
| Heat rejection rate per unit area $\times 10^{-4}$, Btu/(hr)(sq ft) | 1.26 - 3.59 | 1.35 - 3.47 | 1.04 - 3.22 | 1.89 - 2.46 | 1.21 - 2.80 | 2.00 - 4.14 |
| Outlet quality | 0.0 | 0.0 | 0.0 | 0.0 | 0.0 | 0.0 |
| Remarks | Nonwetting | Nonwetting | Nonwetting | Wetting | Wetting | Nonwetting |

TABLE II. - RANGE OF VARIABLES FOR MERCURY CONDENSING

EXPERIMENTS PERFORMED BY HAYS (4)

| Variable | Section 1 | Section 2 | Section 3 |
|---|---|---|---|
| Tube length, in. | 20.0 | 20.0 | 16.25 |
| Tube diameter, in. | 0.072 | 0.150 | 0.157 |
| Tube material | Pyrex | Pyrex | 316 SS |
| Vapor inlet temperature, F | 718 - 740 | 712 - 722 | 675 - 685 |
| Vapor inlet quality | 0.11 - 0.51 | 0.18 - 0.55 | 0.57 - 1.0 |
| Vapor inlet velocity, ft/sec | 40 - 280 | 18 - 91 | 18 - 195 |
| Vapor inlet Reynolds number | 2300 - 16,200 | 2000 - 10,200 | 1700 - 18,400 |
| Mass flow rate, lb/min | 0.258 - 0.450 | 0.305 - 0.482 | 0.076 - 0.472 |
| Heat rejection rate per unit area $\times 10^{-4}$, Btu/(hr)(sq ft) | 7.40 - 11.0 | 1.30 - 3.80 | 0.17 - 2.80 |
| Outlet quality | 0.0 | 0.0 | 0.05 - 1.0 |

TABLE III. - RANGE OF VARIABLES FOR MERCURY CONDENSING

EXPERIMENTS PERFORMED BY ALBERS, ET AL. (10 AND 11)

| Variable | Straight tube | Tapered tube |
|---|---|---|
| Condensing length, in. | 45 - 66 | 45 - 66 |
| Tube diameter, in. | 0.310 | 0.40 - 0.15 |
| Tube material | SS-304 | SS-321 |
| Vapor inlet pressure, psia | 16 - 21 | 14 - 21 |
| Vapor inlet quality | 0.95 - 1.0 | 0.95 - 1.0 |
| Vapor inlet velocity, ft/sec | 180 - 280 | 100 - 180 |
| Vapor inlet Reynolds number | 30,000 - 50,000 | 20,000 - 40,000 |
| Mass flow rate, lb/min | 1.68 - 2.70 | 1.80 - 3.00 |
| Heat rejection rate per unit area, Btu/(hr)(sq ft) | 30,000 - 65,000 | 32,000 - 62,000 |
| Outlet quality | 0.0 | 0.0 |
| Remarks | Nonwetting | Nonwetting |

1. Electrically heated salt bath
2. Mercury pot boiler
3. Superheater section
4. Test section
5. Inlet manometer
6. Manometer manifold
7. Interface control valve
8. Condensate flow meter
9. Reservoir pot
10. Return line
11. Typical test-section pressure taps and manometers
12. Insulation
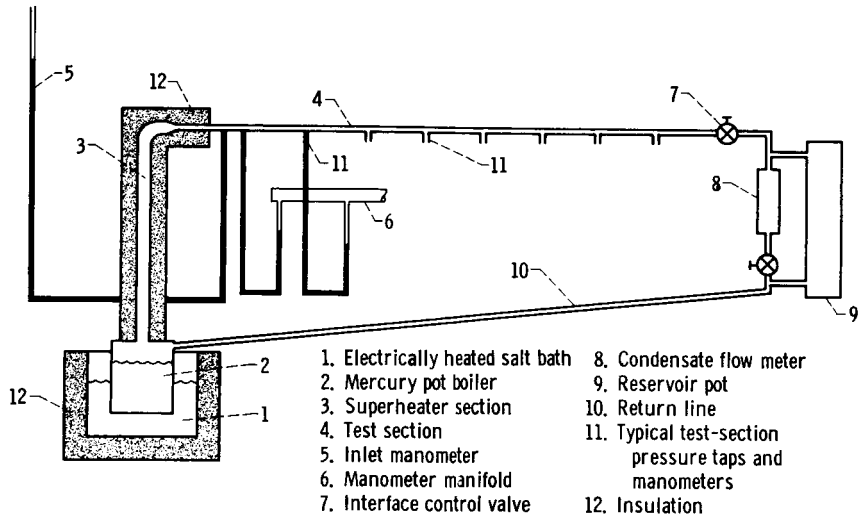
Fig. 1. - Schematic of mercury condensing test rig.
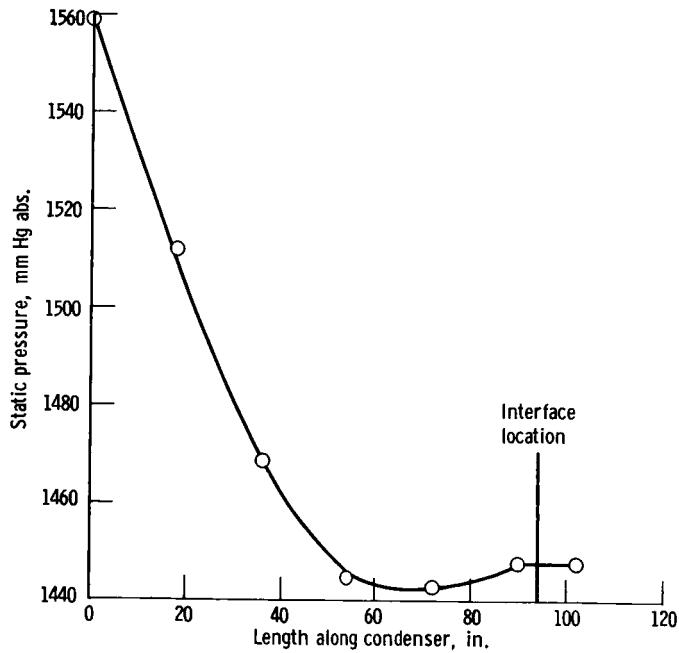


Fig. 2. - Typical static pressure profile. Run A-44.
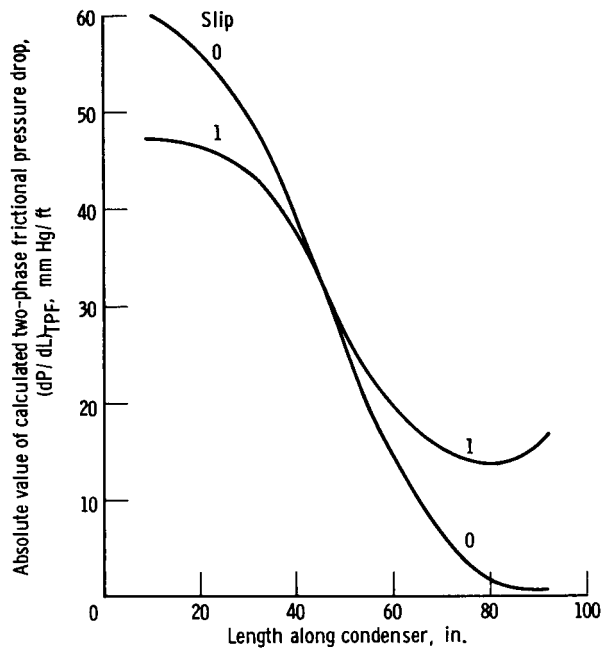
Fig. 3. - Calculated values of two-phase frictional pressure gradients as function of condenser length for slip ratios of zero and one. Run A-44.
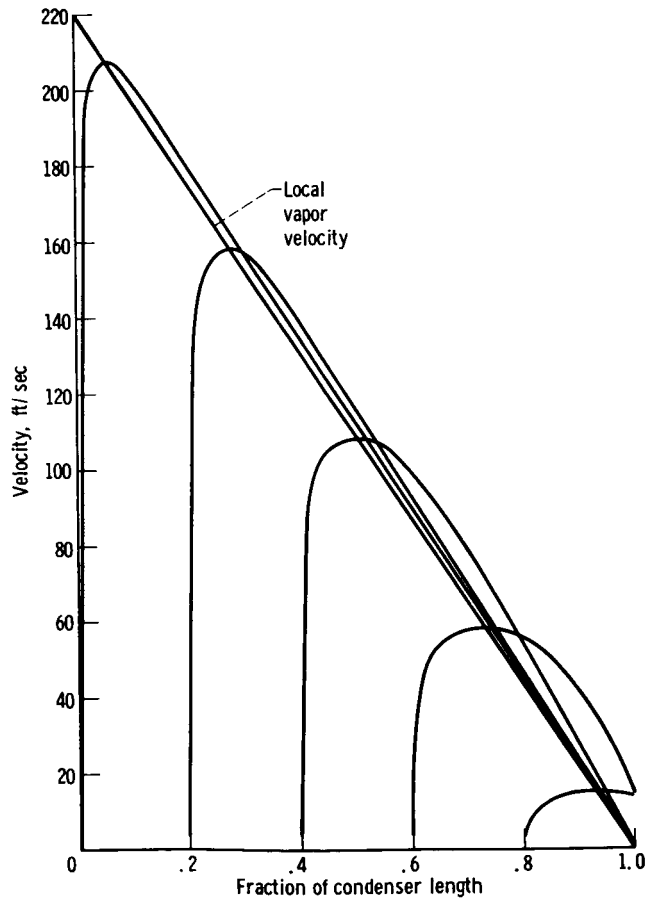


Fig. 4. - Computed local vapor velocity and velocity of mercury drops entrained at various positions along condenser length.
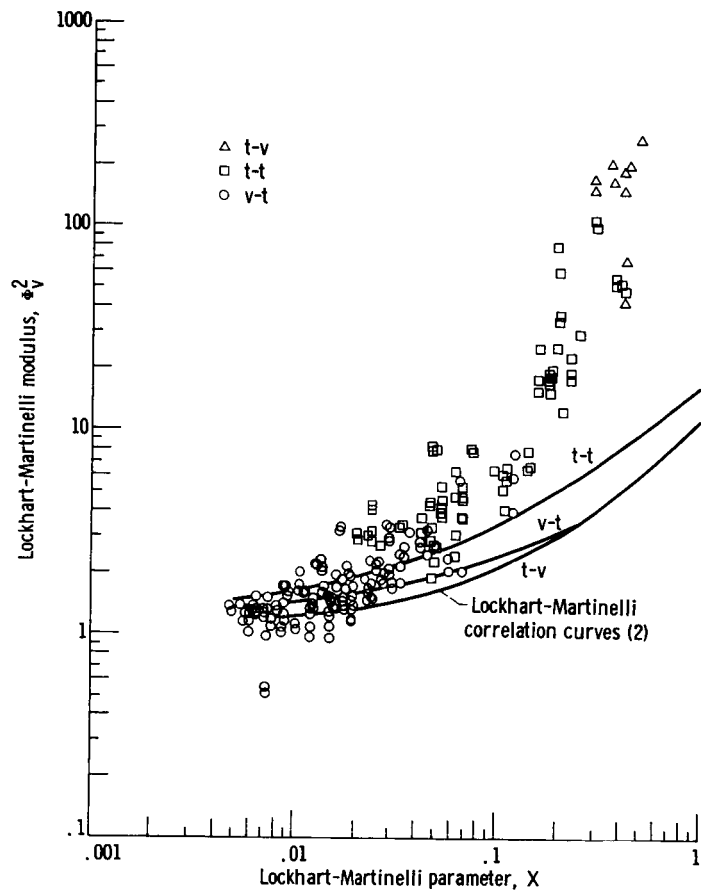
Fig. 5. - Comparison of nonwetting data of Series F with Lockhart-Martinelli correlation.
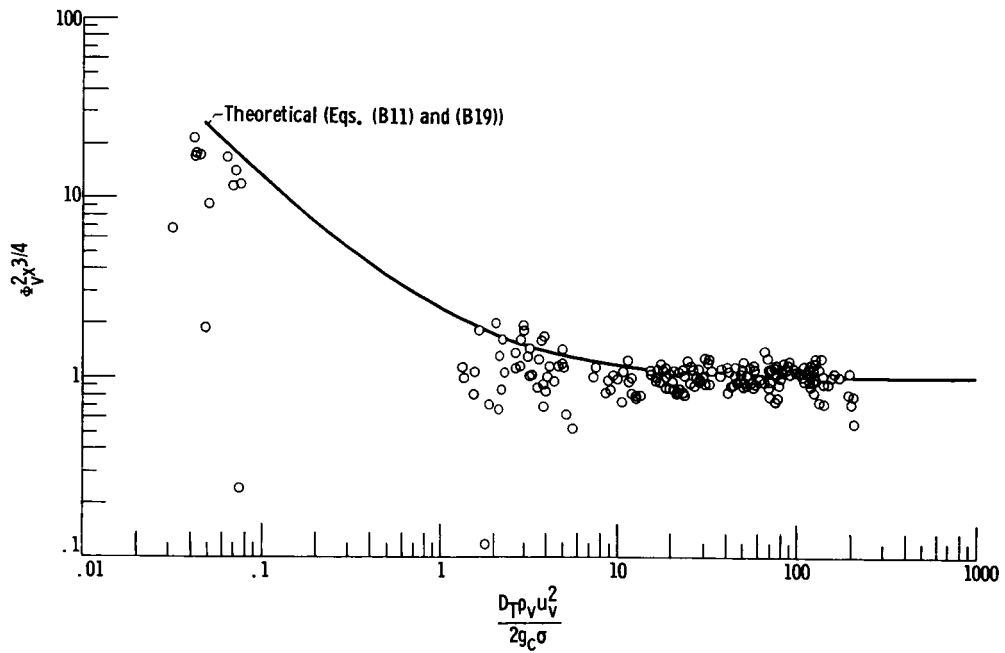


Fig. 6. - Comparison of Series A data with fog-flow prediction.
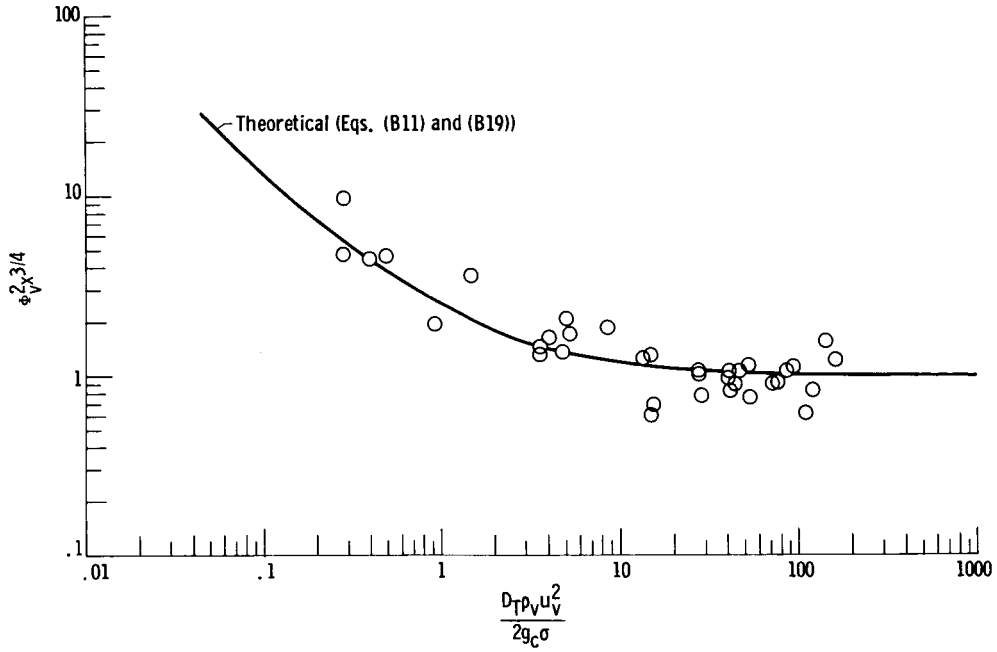
Fig. 7. – Comparison of Series D data with fog-flow prediction.
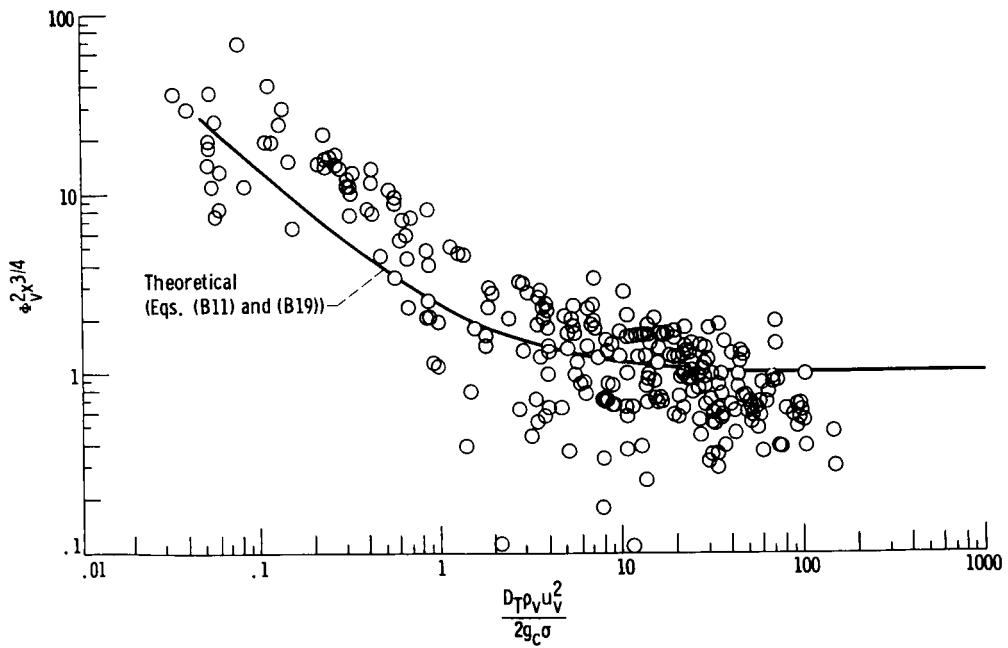


Fig. 8. – Comparison of Series E data with fog-flow prediction.
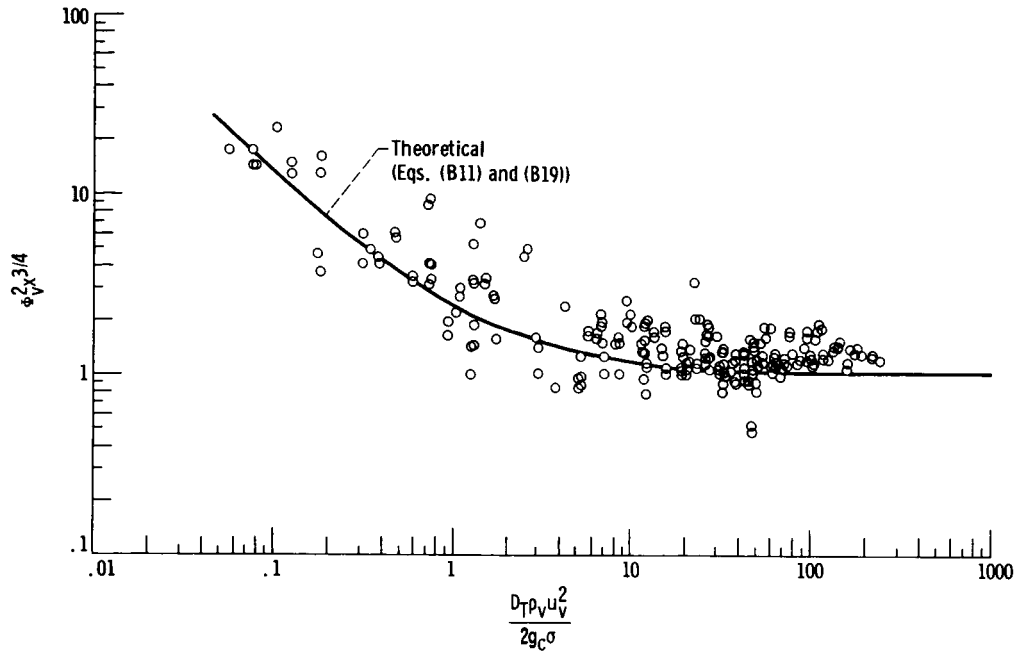
Fig. 9. – Comparison of Series F data with fog-flow prediction.
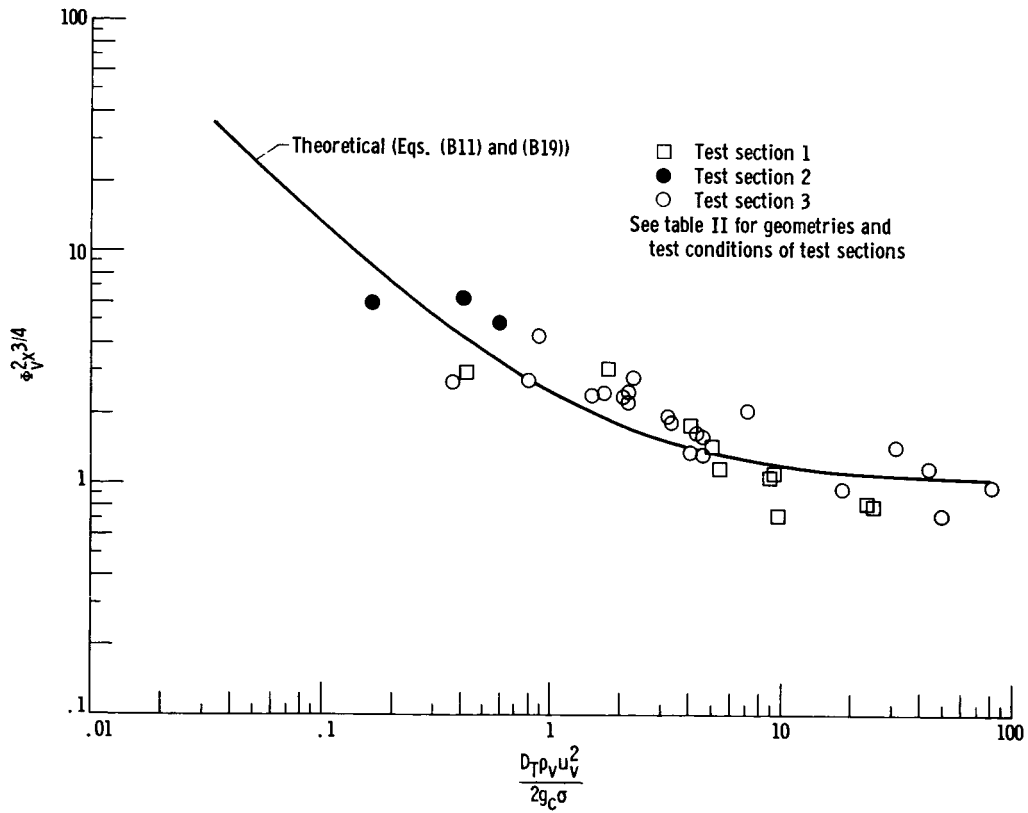


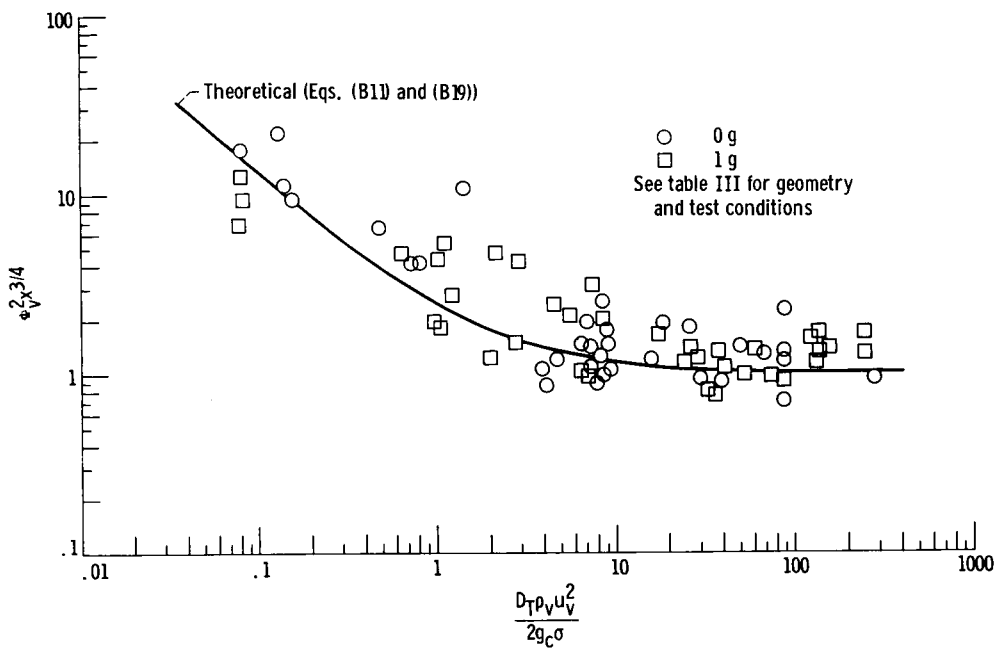Fig. 10. – Comparison of data of Hays (4) with fog-flow prediction.

Fig. 11. – Comparison of mercury condensing data of Albers, et al. (10) with fog-flow theory for constant diameter tube.
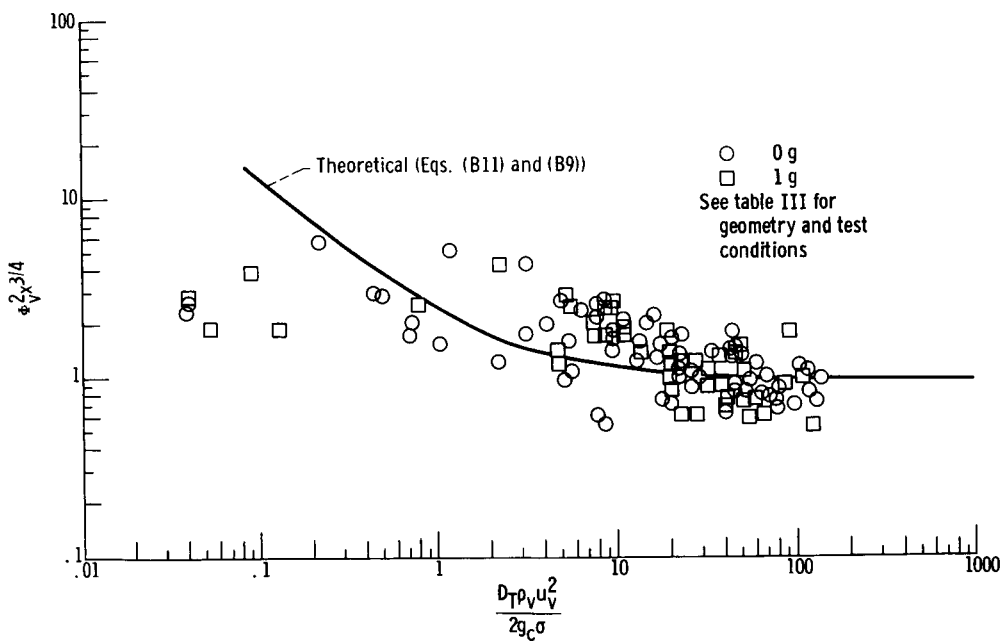


Fig. 12. – Comparison of mercury condensing data of Albers, et al. (11) with fog-flow theory for tapered tube.
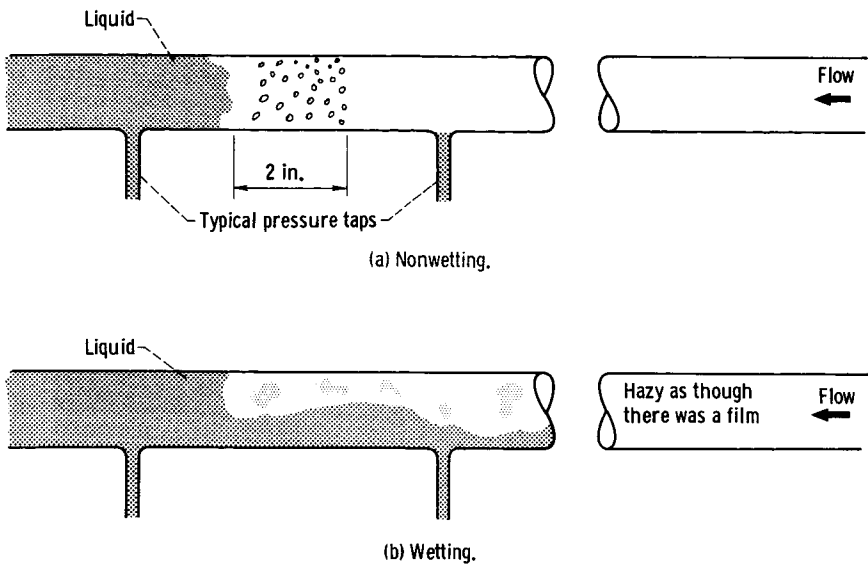
Liquid

Flow

2 in.

Typical pressure taps

(a) Nonwetting.

Liquid

Hazy as though there was a film

Flow

(b) Wetting.

Fig 13. - Schematics of fluoroscopic observations during condensation of mercury in horizontal 316 stainless-steel tube.

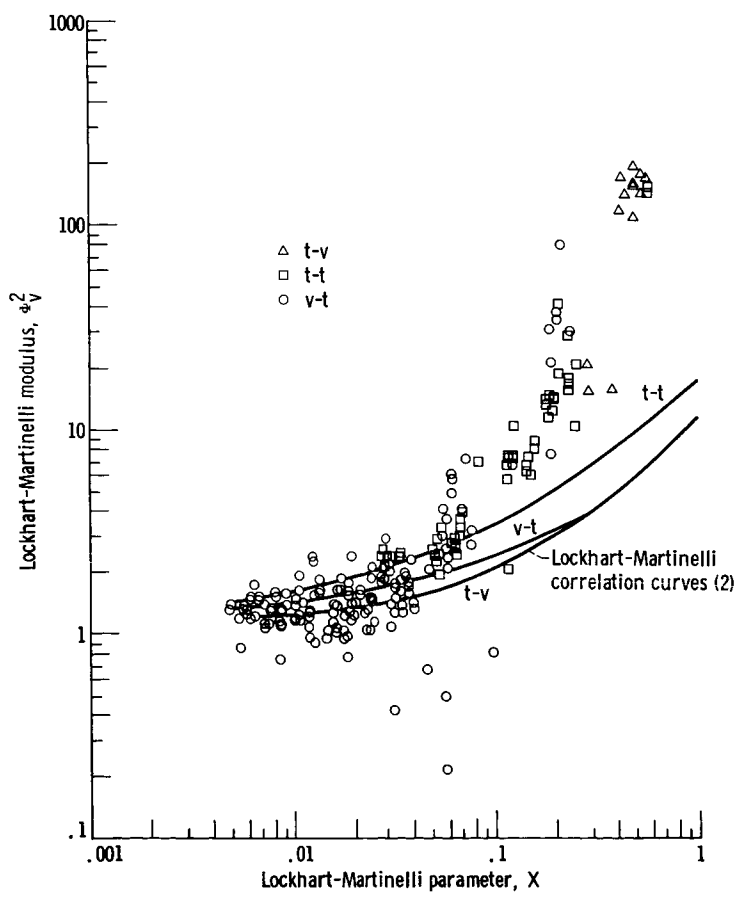Lockhart-Martinelli modulus, $\phi_v^2$

△ t-v
□ t-t
○ v-t

t-t

v-t

Lockhart-Martinelli correlation curves (2)

t-v

Lockhart-Martinelli parameter, X

Fig. 14. - Comparison of wetting data of Series G with Lockhart-Martinelli correlation.
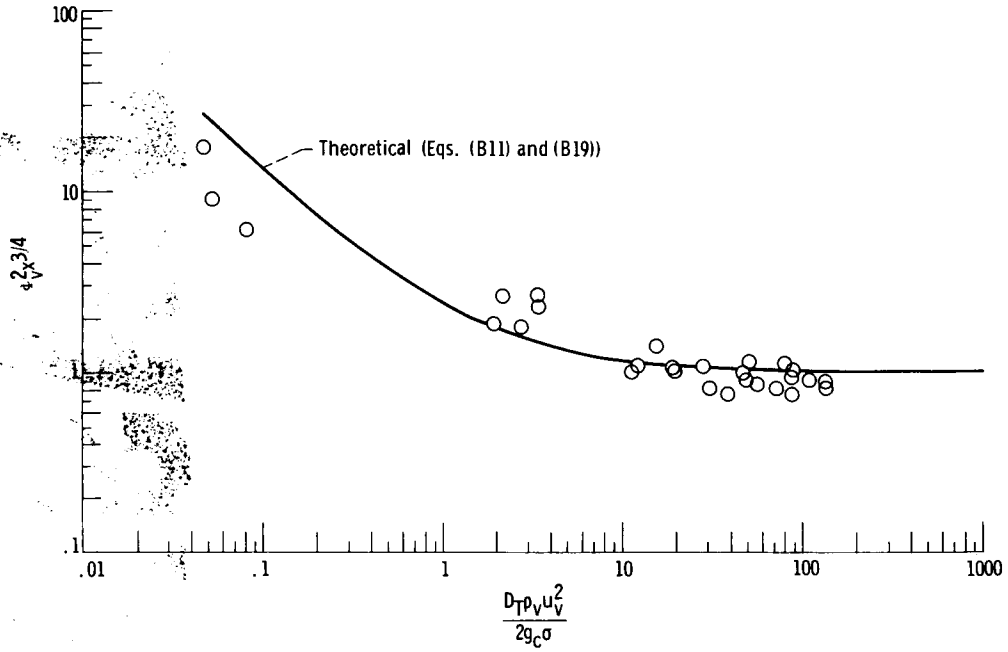
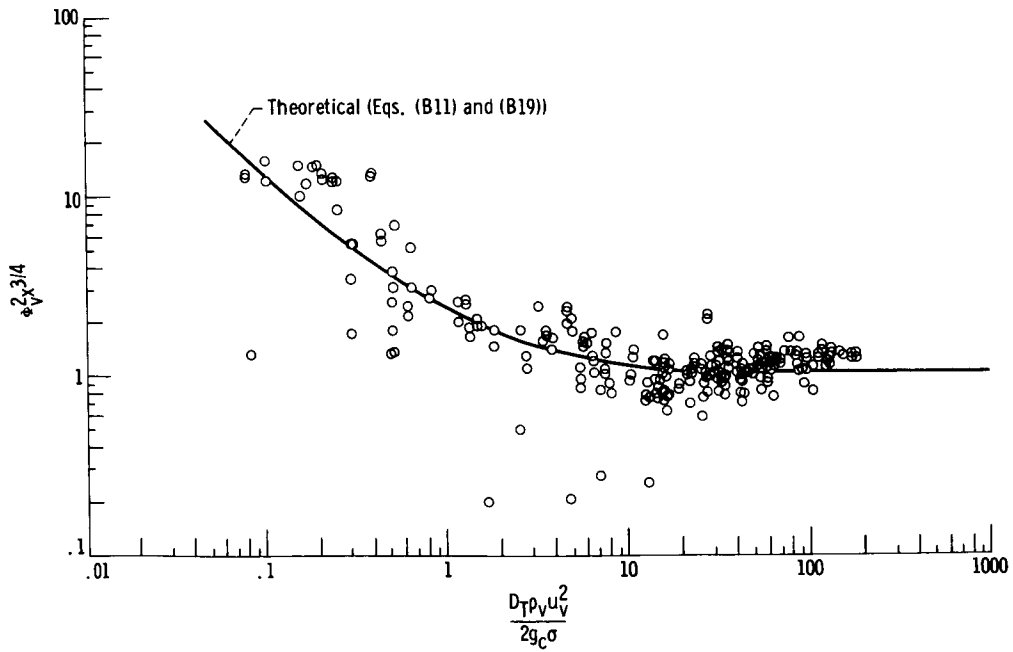Fig. 15. – Comparison of Series W data with fog-flow prediction.



Fig. 16. – Comparison of Series G data with fog-flow prediction.